Atmos. Chem. Phys. Discuss., 10, 13945–13968, 2010
www.atmos-chem-phys-discuss.net/10/13945/2010/
doi:10.5194/acpd-10-13945-2010

Atmospheric Chemistry and Physics Discussions

Constraints on first aerosol indirect effect from a combination of MODIS-CERES satellite data and global climate simulations

X. Ma[1,2], K. von Salzen[2], and J. Cole[2]

[1]School of Earth and Ocean Sciences University of Victoria, Victoria, British Columbia, Canada
[2]Canadian Centre for Climate Modelling and Analysis, Environment Canada, Victoria, British Columbia, Canada

Received: 11 May 2010 – Accepted: 20 May 2010 – Published: 7 June 2010

Correspondence to: K. von Salzen (knut.vonsalzen@ec.gc.ca)

Published by Copernicus Publications on behalf of the European Geosciences Union.

Abstract

Retrievals of cloud top effective radius from MODIS (as derived by CERES) were combined with aerosol concentrations from the CCCma CanAM4 to examine relationships between aerosol and cloud that underlie the first aerosol indirect (cloud albedo) effect. Evidence of a strong negative relationship between sulphate, and organic aerosols, with cloud top effective radius was found for low clouds, indicating both aerosol types are contributing to the first indirect effect on a global scale. Furthermore, effects of aerosol on the cloud droplet effective radius are more pronounced for larger cloud liquid water paths. While CanAM4 broadly reproduces the observed relationship between sulphate aerosols and cloud droplets, it does not reproduce the dependency of cloud top droplet size on organic aerosol concentrations nor the dependency on cloud liquid water path. Simulations with a modified version of the model yield a more realistic dependency of cloud droplets on organic carbon. The robustness of the methods used in the study are investigated by repeating the analysis using aerosol simulated by the GOCART model and cloud top effective radii derived from the MODIS science team.

1 Introduction

The representations of aerosol indirect effects, i.e. aerosol-cloud interactions, remains a source of large uncertainties in GCM simulations of climate change (IPCC, 2007). Representation of aerosol effects on clouds in GCMs range from simple empirical relationships between cloud droplet and aerosol concentrations to more rigorous parameterizations for activation of aerosol particles to cloud droplets.

Twomey (1974) first found that cloud reflectance increases with aerosol particle concentration for constant cloud water content since aerosols can act as cloud condensation nuclei (CCN). This is called the cloud albedo effect, i.e. first indirect effect.

To evaluate the ability of the ECHAM GCM to simulate the first aerosol indirect effect (Lohmann and Lesis, 2002), data from the POLDER satellite was used to examine the

ACPD
10, 13945–13968, 2010

relationship between cloud droplet effective radius and aerosol index (AI). It was found that cloud droplet radius decreased with increasing AI, according to satellite data and model output, and that the relationship was more pronounced in the ECHAM GCM. Again using data from POLDER, Quaas et al. (2004) characterized aerosol impacts on clouds by accounting for variations in cloud liquid water path (LWP). In a later study, Quaas et al. (2008) used data from the Cloud and the Earth's Radiant Energy System (CERES, Wielicki et al., 1996) and the MODerate Resolution Imaging Spectroradiometer (MODIS, Remer et al., 2005) to derive a statistical relationship between cloud properties and column aerosol concentration. This latter study found a much weaker magnitude of the indirect effect compared to other estimates.

An effect of organic carbon on cloud droplet number concentrations and therefore indirect effects is expected from basic Köhler theory. However, the global magnitude of this effect has not yet been determined from global observations.

This study focuses on the effect of sulphate and organic carbon aerosols on low clouds, i.e., clouds with tops below 700 hPa. In the earlier studies described above, the indirect effect was determined using passive measurements that were generally representative of the entire vertical column. By focusing on cloud top droplet effective radius and liquid cloud water path in low clouds from MODIS observations derived by CERES (called MODIS-CE hereafter), outside of the polar regions, one reduces the possibility of retrievals for which there are mixed and ice phase clouds. In addition, aerosol and clouds may occur at different heights in the atmosphere which can obscure local interactions between them. To reduce this possibility, aerosol concentrations within the same height range as low clouds were used, reducing some of the ambiguities caused by using vertically integrated aerosol quantities like the aerosol index.

Furthermore, dry aerosol concentrations, rather than AI, are used to attribute cloud microphysical properties to aerosol properties. This approach eliminates the dependency of the results on hygroscopic growth of aerosol particles. It also reduces possible 3-D radiative transfer effects in the vicinity of clouds on retrieved AI and aerosol optical thickness (Marshak et al., 2008).

ACPD
10, 13945–13968, 2010

2 Model description

Simulations were performed using a developmental version of the CCCma 4th generation atmospheric general circulation model (CanAM4, von Salzen et al., 2005). The spectral resolution of CanAM4 corresponds to a spherical harmonic expansion triangularly truncated at total wave number 63. There are 35 layers in the vertical with a monotonically increasing grid spacing with height, starting at a grid spacing of approximately 100 m near the surface and up to the model top at approximately 1 hPa.

The sea surface temperature (SST) and sea ice boundary conditions in the simulations are from the second phase of the Atmospheric Model Intercomparison Project (Taylor et al., 2000) for the period January 1956 through December 2000, which were averaged to generate the climatological-mean annual cycle for both fields. These were then used to perform 5-year long simulations, with a 5-month spinup period, to generate 5-year climatologies for our analysis.

A bulk aerosol scheme is used in CanAM4, i.e. aerosol size distribution is not prognosed in this version. The prognostic aerosol species in CanAM4 include sulphate, hydrophylic and hydrophobic organic carbon (OC), hydrophylic and hydrophobic black carbon (BC), sea salt, and mineral dust (Lohmann et al., 1999; Croft et al., 2005). Emissions in this study are from the AeroCom (Aerosol Comparison) project for the year 2000 (Textor et al., 2006; Kinne et al., 2006). It provides the aerosol emission data from both natural and anthropogenic sources.

Similar to earlier work by Boucher and Lohmann (1995) and others, the cloud droplet number (N_c) in CanAM4 is empirically related to the concentration of sulphate aerosol (SO_4). Dufresne et al. (2005) adjusted the empirical constants in the parameterization for N_c by fitting GCM results to globally observed results for the cloud droplet effective radius. A slightly modified version of their parameterization is used in CanAM4, based on a comparison between model results and MODIS-CE retrievals for cloud droplet

ACPD
10, 13945–13968, 2010

effective radius giving

$$N_c = 60(SO_4^{0.2}) \quad (1)$$

where N_c is in droplets cm^{-3} and SO_4 in $\mu g\, m^{-3}$. For the simulations, a lower bound of 1 droplet cm^{-3} is used for N_c.

A fully prognostic single-moment cloud micphysics scheme is used in the model, based on the work of Lohmann and Roeckner (1996), Rotstayn (1997) and Khairoutdinov and Kogan (2000). A statistical approach is used for micphysical properties of layer clouds (Chaboureau and Bechtold, 2005). The correlated-k distribution model (Li, 2002; Li and Barker, 2002, 2005) and a more general treatment of radiative transfer in cloudy atmospheres using the McICA methodology (Pincus et al., 2003; Barker et al., 2008) are used in CanAM4.

3 Evaluation of model results using MODIS-CE satellite data

Effects of aerosol on clouds are determined in terms of dry aerosol composition in this study. Observations of dry aerosol composition are only available for a relatively small number of land-based sites around the globe. However, 3-D concentrations for different types of aerosols are available from a number of global models (e.g., AEROCOM project; Textor et al., 2006) While different models can have substantial differences in simulated aerosol life cycles, basic features of simulated aerosol concentration fields are similar for most global aerosol models. For instance, simulated near-surface sulphate concentrations usually vary by several orders of magnitude between polluted regions in the Northern Hemisphere and more remote regions in the Southern Hemisphere, similar to observations (e.g., Chin et al., 1996).

Arguably, large differences in hydrophylic (i.e. cloud-active) accumulation mode aerosol concentrations between different regions should be associated with detectable differences in cloud droplet sizes following the first aerosol indirect effect. For example, relationships between cloud droplet effective radius in low clouds and associated aerosol concentrations can be obtained from GCMs. They may also be obtained by

ACPD
10, 13945–13968, 2010

combining long-term simulated aerosol concentrations and long-term satellite-based retrievals of cloud droplet effective radius. For sufficiently long averaging time periods, weather-related variations of accumulation mode aerosol and cloud properties can be expected to be small compared to climatological features.

There are several possibilities to compare cloud top effective radii simulated by GCMs with satellite-based retrievals. For example, some studies simply used the cloud droplet radius from the uppermost model layer containing liquid water (Quaas et al., 2004). For this study, a slightly more sophisticated approach is taken by instead using a modified version of the ISCCP simulator (Klein and Jacob, 1999) which emulates cloud-related variables comparable with data provided by MODIS-CE. These include cloud amount, cloud top pressure, cloud optical thickness, cloud water path and cloud top effective radius for clouds in the four pressure ranges used by MODIS-CE.

Seasonal mean results for the time period June, July and August (JJA), and December, January and February (DJF) are used for the study. Results for JJA only are shown in the paper.

4 Aerosol concentrations and cloud effective radius

The CanAM4 simulated sulphate (SO_4) and hydrophilic organic carbon (OC) concentrations at low level (surface to 700 hPa) are shown in Fig. 1. For sulphate, concentration maxima over North America, Europe, and Asia are mainly due to emissions from industrial fossil fuel burning. Secondary maxima are found downwind of major emission sources and South America because of biomass burning. Results for OC are dominated by biomass burning emissions from South America and South Africa.

The cloud top effective radius (r_{eff}) retrieved from MODIS-CE for low clouds is shown in Fig. 2 (left panel). Large cloud droplets are mainly found over the ocean, where aerosol particle concentrations are low and cloud liquid water contents are high, while cloud droplets are smaller over land. Very large values over Africa could be caused by less accurate retrieval over bright and dust-laden deserts, and will be excluded in this study.

ACPD
10, 13945–13968, 2010

Similar to the observations, the simulated cloud effective radius from CanAM4 in Fig. 2 (right panel) is characterized by large values over the ocean and smaller values over land. However, the modelled r_{eff} is generally smaller than the MODIS-CE retrievals over the Southern ocean, but larger than the MODIS-CE retrievals in the Northern Hemisphere.

5 Dependency of cloud droplet size on dry aerosol concentration

Figure 3 shows relationships between cloud top effective radius and dry aerosol concentrations in JJA for low clouds with tops below 700 hPa using data from all grid points in the MODIS-CE and model data sets between 65° S and 65° N. The same resolution (128×64 grid points) is used for both data sets. Data from high latitudes is excluded due to potential difficulties retrieving cloud microphysical properties over bright surface conditions, such as snow and sea ice, as well as in potentially more frequent mixed-phase cloud conditions.

According to Fig. 3, r_{eff} decreases with increasing concentrations of SO_4 for both MODIS-CE and the GCM (upper panel). This behaviour is broadly consistent with relationships between cloud droplet size and aerosol index from previous studies (Lohmann and Lesis, 2002; Quaas et al., 2008). Cloud top droplet size from MODIS-CE also decreases with increasing concentrations of hydrophylic OC, indicating a potential contribution of OC to the first indirect effect. Interestingly, simulated results for r_{eff} also yield a slight decrease in size with OC although there is no contribution of OC to cloud droplet number according to Eq. (1). Apparently the relatively simple analysis above is not sufficient for detecting potential effects of OC on cloud droplets because correlations between OC and SO_4 are not accounted for.

In order to determine relative contributions of SO_4 and OC to the first indirect effect more accurately, results for r_{eff} were further stratified using cloud liquid water content (Figs. 4 and 5). According to Twomey (1974), increased concentrations of atmospheric aerosol will result in higher concentrations of cloud condensation nuclei (CCN),

ACPD
10, 13945–13968, 2010

increased cloud droplet concentrations, and therefore smaller droplets. The hypothesis underlying the first indirect effect applies to clouds of equal liquid water content (LWC). Although important, this was largely omitted in previous studies of indirect effects using satellite-based data, mainly due to observational constraints.

Figure 4 shows relationships between r_{eff} and SO_4, for which the data for r_{eff} and SO_4 were stratified according to three LWP categories, using simulated results for the LWP from the model. Furthermore, in order to distinguish the contributions from SO_4 and OC, the data were also stratified according to three categories of OC in each LWP category. The linear regression results by least square for each category are also shown. For all LWP and OC categories, r_{eff} decreases with increasing concentration of SO_4 (except for the case with low LWP and large OC, there is a slightly increase). The mean slope from CanAM4 for $d\log(r_{reff})/d\log(SO_4)$ is close to −0.05, with a range from −0.03 to −0.06, which is in reasonably good agreement with the theoretical value of −0.067 according to Eq. (1). On the other hand, the diagnosed slope for the MODIS-CE results is in the range from −0.01 to −0.17, indicating that the observed relationship between aerosol and cloud is fundamentally more complex than assumed in the model. Model results and observations agree well at intermediate values of the LWP and OC concentrations. The model tends to overestimate the dependency of the cloud droplet size on SO_4 at low LWP and underestimate it at high LWP.

Figure 5 is similar to Fig. 4, except results are shown for OC instead of SO_4. Results for r_{eff} from CamAM4 do not show any significant increase or decrease with OC concentrations, with a diagnosed slope around zero, as theoretically expected from Eq. (1). However, the slope is negative for MODIS-CE results, with values ranging from 0 to −0.09. According to these results, effects of OC on cloud droplet size are potentially of the same order of magnitude as effects of SO_4. This effect is apparently missing in the model.

In order to summarize the findings described above, the data were stratified into more categories, i.e. ten categories for sulphate ranging from 0.1 to 100.0 mg/m^2 and OC concentrations ranging from 0.01 to 10.0 mg/m^2. The dependency of r_{eff} on SO_4 and

ACPD
10, 13945–13968, 2010

OC is shown in Fig. 6. As shown before, simulated values of r_{eff} generally decrease with increasing sulphate concentration with no obviously systematic dependency on OC concentration. In contrast, MODIS-CE retrieved r_{eff} clearly decreases with increasing aerosol concentrations. In particular, there is a clear dependency of r_{eff} on OC according to MODIS-CE results, giving evidence for a substantial contribution of OC to the first indirect effect. The omission of this effect in the CanAM4 is evident for all LWP categories, indicating a shortcoming of the parameterized effect of aerosols on clouds.

6 Robustness of results

In order to determine the robustness of our analysis, simulated aerosol concentrations from GOCART (Chin et al., 2001) for the period 2001–2005 were used instead of aerosol concentrations from CanAM4. The GOCART model is a global model with a horizontal resolution of 144×91 grid points and 31 vertical levels. It uses a bulk scheme to model sulphate as well as hydrophylic and hydrophobic BC and OC. A bin scheme is used to model size distributions for sea salt and mineral dust. Assimilated meteorological fields from the NASA Goddard Earth Observing System Data Assimilation System (GEOS DAS) is provided to GOCART.

Retrieved values of r_{eff} from MODIS-CE in combination with aerosol concentrations from GOCART are shown in Fig. 6 (third panel). Overall, there is good agreement with the results using aerosol concentrations from CanAM4 and MODIS-CE r_{eff}, i.e. a strong anti-correlation is also found between OC and r_{eff}.

This study focused on cloud top effective radius retrieved by MODIS-CE and extracted from CanAM4, while aerosol concentrations from CanAM4 simulations only. Since there are uncertainities associated with satellite retrievals of cloud properties, climatological results retrieved from MODIS science team (MODIS-ST hereafter) for low clouds in JJA, averaged over 2001–2005, are also used in our analysis. Like the MODIS-CE data, level 3 MODIS data from Terra was used (Hubanks et al., 2008). Figure 7, compares the climatological zonal mean cloud top effective radius from

ACPD
10, 13945–13968, 2010

CanAM4, MODIS-CE and MODIS-ST for clouds with cloud top pressure greater than 700 hPa. The differences between the MODIS-CE and MODIS-ST retrieved values can in part be attributed to differing retrievals (Minnis et al., 2010) and provide a sense of the observational range relative to what is diagnosed from CanAM4. There is broad agreement between CanAM4, MODIS-CE and MODIS-ST, cloud effective radius indicates the latitudinal increase from north to south although there is a clear difference poleward of 30° N with CanAM4 systematically simulating cloud top effective radii that are too large relative to MODIS-ST and MODIS-CE. The CanAM4 also simulates a somewhat weaker change between the Northern and Southern Hemisphere.

In order to investigate the impact of uncertainties in satellite retrievals of cloud top effective radius on the results, the analysis described above was repeated replacing MODIS-CE retrievals of r_{eff} with MODIS-ST. The results are shown in the bottom panel of Fig. 6. Although there can be large differences between the MODIS-ST and MODIS-CE retrievals of cloud top effective radius, the dependency of r_{eff} on aerosol concentrations is similar for both data sets.

7 Model modifications

Results presented in the previous section give evidence for the need to include effects of OC on cloud droplets in climate models. A slightly more complex parameterization for cloud droplet number concentration, which includes effects of OC and sea salt aerosol, was proposed by Menon et al. (2001). Accordingly, the relationships below are used in an additional simulation with a modified version of CanAM4 to predict cloud droplet number N_{c} for land, N_{land} and ocean, N_{ocean}.

$$N_{\mathrm{land}} = 10^{2.41+0.50\log(\mathrm{SO_4})+0.13\log(\mathrm{OM})} \tag{2}$$

$$N_{\mathrm{ocean}} = 10^{2.41+0.50\log(\mathrm{SO_4})+0.13\log(\mathrm{OM})+0.05\log(\mathrm{Seasalt})} \tag{3}$$

where OM refers to the concentration of organic matter (OM=1.4 OC).

ACPD
10, 13945–13968, 2010

Results from this simulation are shown in Figs. 8 and 9. In contrast to the results from the original CDNC parameterization, r_{eff} decreases too strongly with increasing SO_4. However, there is good agreement between model results and observations for the dependency of r_{eff} on OC.

This indicates that the first indirect effect from SO_4 is higher with the parameterization by Menon et al. than in the original simulation. Overall, contributions of OC to the first indirect effect are well reproduced by this parameterization. However, it should be noted that in the limiting case of vanishing OC, the parameterized cloud droplet number concentration according to Eqs. (2) and (3) is nil, independent of the amount of sulphate. It is unclear how this somewhat counterintuitive behaviour may have affected the results in Figs. 8 and 9.

8 Conclusions

Robust decreases in cloud top droplet effective radius with increasing concentrations of simulated sulphate and OC aerosol were found for low clouds based on a combination of satellite data and GCM results. This is consistent with the hypothesis underlying the first indirect effect. Results presented in this study suggest that OC may have similar efficiency in affecting cloud droplet sizes as sulphate on a global scale. This indicates a potentially large contribution of OC to the first indirect effect.

The CCCma CanAM4 produces relationships between cloud droplet size and sulphate concentrations that are similar, giving evidence for an overall realistic representation of the first indirect effect due to sulphate aerosol on a global scale. However, the model does not reproduce a decrease in cloud droplet sizes with increasing OC concentrations found when using satellite-based retrievals of cloud droplet sizes. The GCM results also have less dependency on cloud liquid water path; namely that the magnitude of the first indirect effect increases with LWP for observed cloud droplet sizes from MODIS-CE.

ACPD
10, 13945–13968, 2010

A modified version of CanAM4 which accounts for a contribution of OC to cloud droplet number (Menon et al., 2001) produced good agreement of model results with MODIS-CE retrievals for the dependency of the droplet size on OC concentrations.

At this point it is not clear what causes the increase in the magnitude of the first indirect effect with increasing cloud water path. However, it is possible that cloud dynamics can lead to differences in the magnitude of the first aerosol indirect effect (Feingold, 2003). For example, larger updraft velocities in convective clouds likely lead to a stronger first indirect effect compared to lower updraft velocities in stably stratified stratiform clouds. The parameterization of cloud droplet number concentration currently employed in CanAM4 does not account for differences in cloud dynamics.

Relationships between cloud droplet effective radius and dry aerosol concentrations will be used in future comparisons of GCM simulations with a more detailed representation of aerosol and cloud microphysical processes. For example, a future version of the CCCma CanAM4 will include a parameterization for the activation of aerosol that accounts for contributions from sulphate, OC and other aerosol types.

Acknowledgements. We thank Mian Chin for providing GOCART model results. We also thank two internal reviewers (John Fyfe and Kirsten Zickfeld) for their helpful comments and suggestions. MODIS-CERES data were obtained from the NASA Langley Research Center EOSDIS Distributed Active Archive Center and MODIS Science Team data were retrieved from the NASA Level 1 and Atmosphere Archive and Distribution System (LAADS). Funding for this study has been provided by the Canadian Foundation for Climate and Atmospheric Sciences (CFCAS) via the Cloud/Aerosol Feedbacks and Climate research network (CAFC) and Environment Canada.

References

Barker, H. W., Cole, J. N. S., Morcrette, J. J., Pincus, R., Raisanen, P., von Salzen, K., and Vaillancourt, P. A.: The Monte Carlo Indepedent Column Approximation: an assessment using several global atmospheric models, Q. J. Roy. Meteor. Soc., 134, 1463–1478, 2008. 13949

ACPD
10, 13945–13968, 2010

Boucher, O. and Lohmann, U.: The sulfate-CCN-cloud albedo effect: a sensitivity study with two general circulation models, Tellus B, 47, 281–300, 1995. 13948

Chaboureau, J.-P. and Bechtold, P.: Statistical representation of clouds in a regional model and the impact on the diurnal cycle of convection during tropical convection, cirrus and nitrogen oxides (TROCCINOX), J. Geophys. Res., 110, D17103, doi:10.1029/2004JD005645, 2005. 13949

Chin, M., Jacob, D. J., Gardber, G. M., Spiro, P. A., Foreman-Fowler, M., and Savoie, D. L.: A global three-dimensional model of tropospheric sulfate, J. Geophys. Res., 101, 18667–18690, 1996. 13949

Chin, M., Ginoux, P., Kinne, S., Torres, O., Holben, B. N., Duncan, B. N., Martin, R. V., Logan, J. A., and Higurashi, A.: Tropospheric aerosol optical thickness from GOCART model and comparisons with satellite and sun photometer measurements, J. Atmos. Sci., 59, 461–483, 2001. 13953

Croft, B., Lohmann, U., and von Salzen, K.: Black carbon ageing in the Canadian Centre for Climate modelling and analysis atmospheric general circulation model, Atmos. Chem. Phys., 5, 1931–1949, doi:10.5194/acp-5-1931-2005, 2005. 13948

Feingold, G.: Modeling of the first indirect effect: analysis of measurement requirements, Geophys. Res. Lett., 30(19), 1997, doi:10.1029/2003GL017967, 2003. 13956

Hubanks, P., King, M., Platnick, S., and Pincus, R.: MODIS Atmosphere L3 Gridded Product Algorithm Theroretical Basis Document, ATBD, Reference Number: ATBD-MOD-30, 2008. 13953

IPCC: Contribution of Working Group I to the Fourth Assessment report of the intergovernment panel on climate change, Cambridge University Press, 2007. 13946

Khairoutdinov, M. and Kogan, Y.: A new cloud physics parameterization in a large-scale simulation model of marine stratocumulus, Mon. Weather Rev., 128, 229–243, 2000. 13949

Kinne, S., Schulz, M., Textor, C., Guibert, S., Balkanski, Y., Bauer, S. E., Berntsen, T., Berglen, T. F., Boucher, O., Chin, M., Collins, W., Dentener, F., Diehl, T., Easter, R., Feichter, J., Fillmore, D., Ghan, S., Ginoux, P., Gong, S., Grini, A., Hendricks, J., Herzog, M., Horowitz, L., Isaksen, I., Iversen, T., Kirkevåg, A., Kloster, S., Koch, D., Kristjansson, J. E., Krol, M., Lauer, A., Lamarque, J. F., Lesins, G., Liu, X., Lohmann, U., Montanaro, V., Myhre, G., Penner, J., Pitari, G., Reddy, S., Seland, O., Stier, P., Takemura, T., and Tie, X.: An AeroCom initial assessment – optical properties in aerosol component modules of global models, Atmos. Chem. Phys., 6, 1815–1834, doi:10.5194/acp-6-1815-2006, 2006.

13948
Klein, S. A. and Jacob, C.: Validation and sensitivities of frontal clouds simulated by the ECMWF model, Mon. Weather Rev., 127(10), 2514–2531, 1999. 13950
Li, J.: Accounting for unresolved clouds in a 1D infrared radiative transfer model. Part 1: Solution for radiative transfer, including cloud scattering and overlap, J. Atmos. Sci., 59, 3302–3320, 2002. 13949
Li, J. and Barker, H. W.: Accounting for unresolved clouds in a 1D infrared radiative transfer model. Part 2: Horizontal variability of cloud water path, J. Atmos. Sci., 59, 3321–3339, 2002. 13949
Li, J. and Barker, H. W.: A radiation algorithm with correlated-k distribution. Part 1: Local thermal equilibrium, J. Atmos. Sci., 62, 286–309, 2005. 13949
Lohmann, U. and Lesis, G.: Stronger constriants on the anthropogenic indirect aerosol effect, Science, 298, 1012–1015, 2002. 13946, 13951
Lohmann, U. and Roeckner, E.: Design and performance of a new cloud micphysics scheme developed for the ECHAM general circulation model, Clim. Dynam., 12, 557–572, 1996. 13949
Lohmann, U., von Salzen, K., McFarlane, N., Leighton, H. G., and Feichter, J.: Tropospheric sulphur cycle in the Canadian General Circulation Model, J. Geophys. Res., 104, 26833–26858, 1999. 13948
Marshak, A., Wen, G., Coakley, J., Remer, L., Loeb, N. G., and Cahalan, R. F.: A simple model for the cloud adjacency effect and the apparent bluing of aerosols near clouds, J. Geophys. Res., 113, D14S17, doi:10.1029/2007JD009196, 2008. 13947
Menon, S., Genio, A. D., Koch, D., and Tselioudis, G.: GCM Simulations of the Aerosol Indirect Effect: Ssensitivity to Ccloud Parameterization and Aerosol Burden, J. Atmos. Sci., 59, 692–713, 2001. 13954, 13956
Minnis, P., Sun-Mack, S., Chen, Y., Khaiyer, M. M., Yi, Y., K.Ayers, J., Brown, R. R., Dong, X., Gibson, S. C., Heck, P. W., Lin, B., Nordeen, M. L., Nguyen, L., Palikonda, R., Smith, W. L., Spangenberg, D. A., Trepte, Q. Z., and Xi, B.: CERES Edition-2 Cloud Property Retrievals Using TRMM VIRS and TERRA and AQUA MODIS Data, Part 2: Examples of average results and comparisons with other data, IEEE T. Geosci. Remote Sens., in review, February 2010. 13954
Pincus, R., Barker, H. W., and Morcrette, J. J.: A fast, flexible, approximate technique for computing radiative transfer in inhomogeneous cloud fields, J. Geophys. Res., 110,

ACPD
10, 13945–13968, 2010

doi:10.1029/202JD003322, 2003. 13949
Quaas, J., Boucher, O., and Breon, F. M.: Aerosol indirect effects in POLDER satellite data and the Laboratoire de Meteorologie Dynamique-Zoom (LMDZ) general circulation model, J. Geophys. Res., 109, D08205, doi:10.1029/2003JD004317, 2004. 13947, 13950
Quaas, J., Bofeinucher, O., Bellouin, N., and Kinne, S.: Satellite-based estimate of the direct and indirect aerosol climate forcing, J. Geophys. Res., 113, doi:10.1029/2007JD008962, 2008. 13947, 13951
Remer, L., Kaufman, Y., Tanre, D., Mattoo, S., Chu, D., Martin, J., Li, R.-R., Ichoku, C., Levy, R., Kleidman, R., Eck, T., Vermote, E., and Holben, B.: The MODIS aerosol algorithm, products and validation, J. Atmos. Sci., 62(4), 947–973, 2005. 13947
Rotstayn, L.: A physically based scheme for the treatment of stratiform clouds and precipitation in large-scale models. Part 1: Description and evaluation of the micphysical processes., Q. J. Roy. Meteor. Soc., 123, 1227–1282, 1997. 13949
Taylor, K. E., Williamson, D., and Zwiers, F.: The sea surface temperature and sea-ice concentration boundary conditions for AMIP II simulations, PCMDI report No. 60, in: Program for Climate Model Diagnosis and Intercomparison, university of California, Lawrence Livermore National Laboratory, Livermore, California, 28 pp., 2000. 13948
Textor, C., Schulz, M., Guibert, S., Kinne, S., Balkanski, Y., Bauer, S., Berntsen, T., Berglen, T., Boucher, O., Chin, M., Dentener, F., Diehl, T., Easter, R., Feichter, H., Fillmore, D., Ghan, S., Ginoux, P., Gong, S., Grini, A., Hendricks, J., Horowitz, L., Huang, P., Isaksen, I., Iversen, I., Kloster, S., Koch, D., Kirkevåg, A., Kristjansson, J. E., Krol, M., Lauer, A., Lamarque, J. F., Liu, X., Montanaro, V., Myhre, G., Penner, J., Pitari, G., Reddy, S., Seland, Ø., Stier, P., Takemura, T., and Tie, X.: Analysis and quantification of the diversities of aerosol life cycles within AeroCom, Atmos. Chem. Phys., 6, 1777–1813, doi:10.5194/acp-6-1777-2006, 2006. 13948, 13949
Twomey, S.: Pollution and the planery albedo, Atmos. Environ., 8, 1251–1256, 1974. 13946, 13951
von Salzen, K., McFarlane, N. A., and Lazare, M.: The role of shallow convection in the water and energy cycles of the atmosphere, Clim. Dynam., 25, 671–699, doi:10.1007/s00382-005-0051-2, 2005. 13948
Wielicki, B., Barkstrom, B., Harrison, E., Lee, R., Smith, G., and Cooper, J.: Clouds and the Earth's Radiant Energy System (CERES): An Earth Observing System experiment, B. Am. Meteorol. Soc., 77, 853–868, 1996. 13947

ACPD
10, 13945–13968, 2010

Constraints on first indirect effect of aerosols

X. Ma et al.

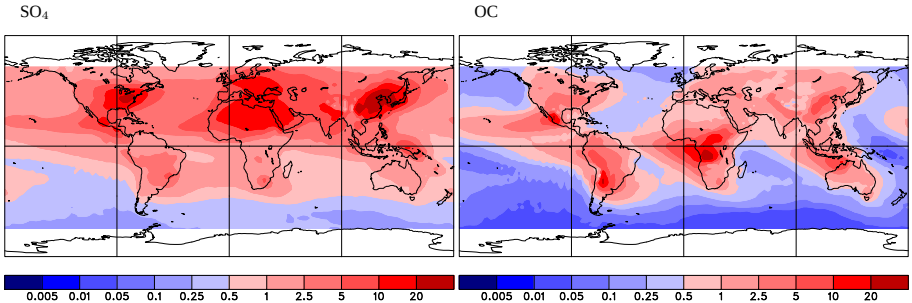

Fig. 1. Vertically-integrated sulphate (SO_4) and hydrophylic organic carbon (OC) concentrations for low level (surface to 700 hPa) in JJA from CanAM4 simulations. Unit: mg/m^2.

ACPD
10, 13945–13968, 2010

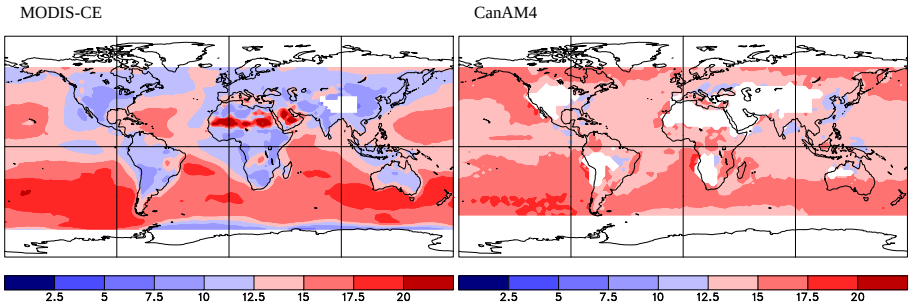

Fig. 2. Cloud top effective radius from MODIS-CE and CanAM4 for low level (surface to 700 hPa) in JJA. Unit: µm.

ACPD
10, 13945–13968, 2010

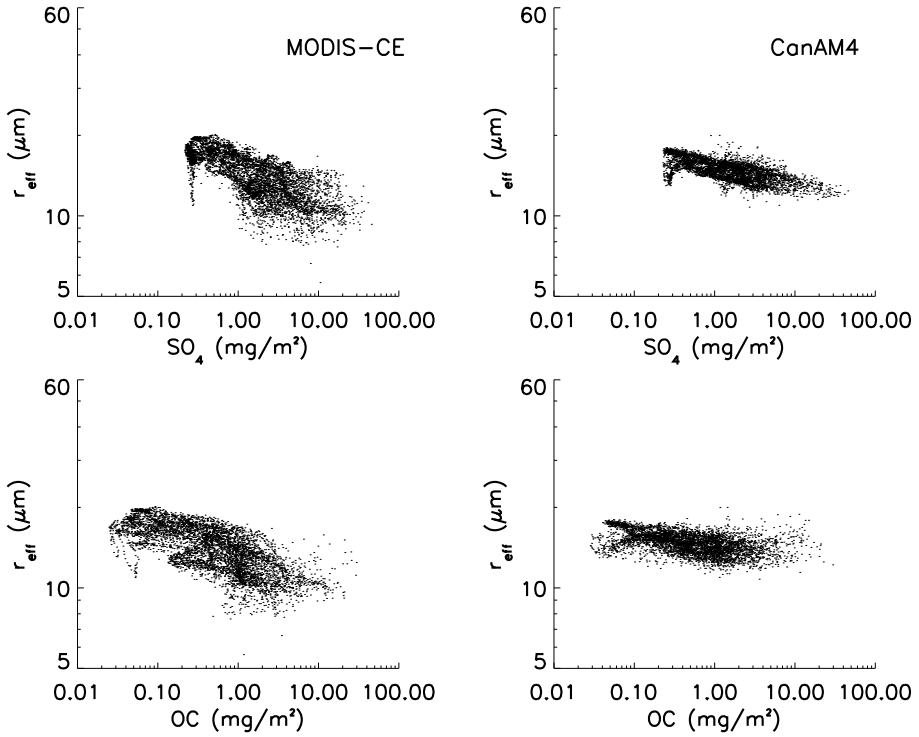

Fig. 3. Cloud effective radius (r_{eff}) versus aerosol concentrations in JJA for low level (surface to 700 hPa). The concentrations of sulphate (SO_4) and hydrophylic organic carbon (OC) are taken from the CanAM4 simulations while r_{eff} is from MODIS-CE retrievals (left column) and CanAM4 (right column).

ACPD
10, 13945–13968, 2010

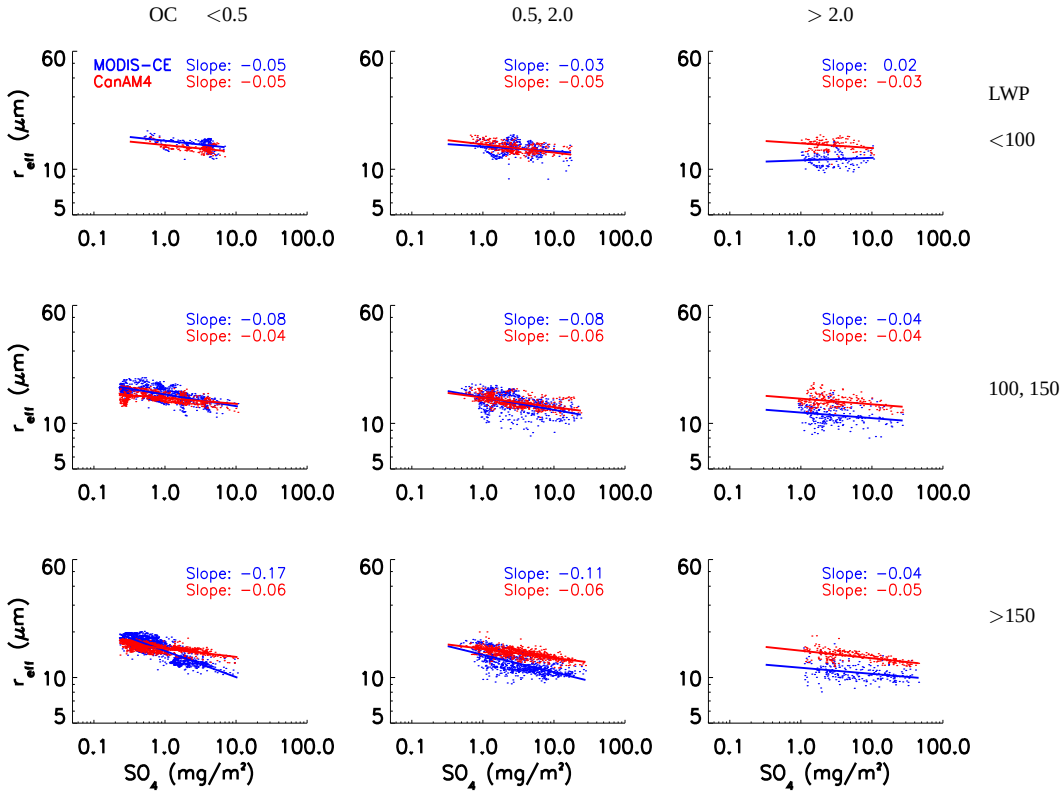

Fig. 4. Low (surface to 700 hPa) cloud effective radius (in μm) from MODIS-CE (in blue) and CanAM4 (in red) versus sulphate (SO_4) concentrations in JJA. The data were stratified for 3 categories of liquid water path (LWP, in g/m^2), and 3 categories of hydrophylic organic carbon (OC, in mg/m^2). The slope from linear regression are also marked in the plots.

ACPD
10, 13945–13968, 2010

Constraints on first indirect effect of aerosols

X. Ma et al.

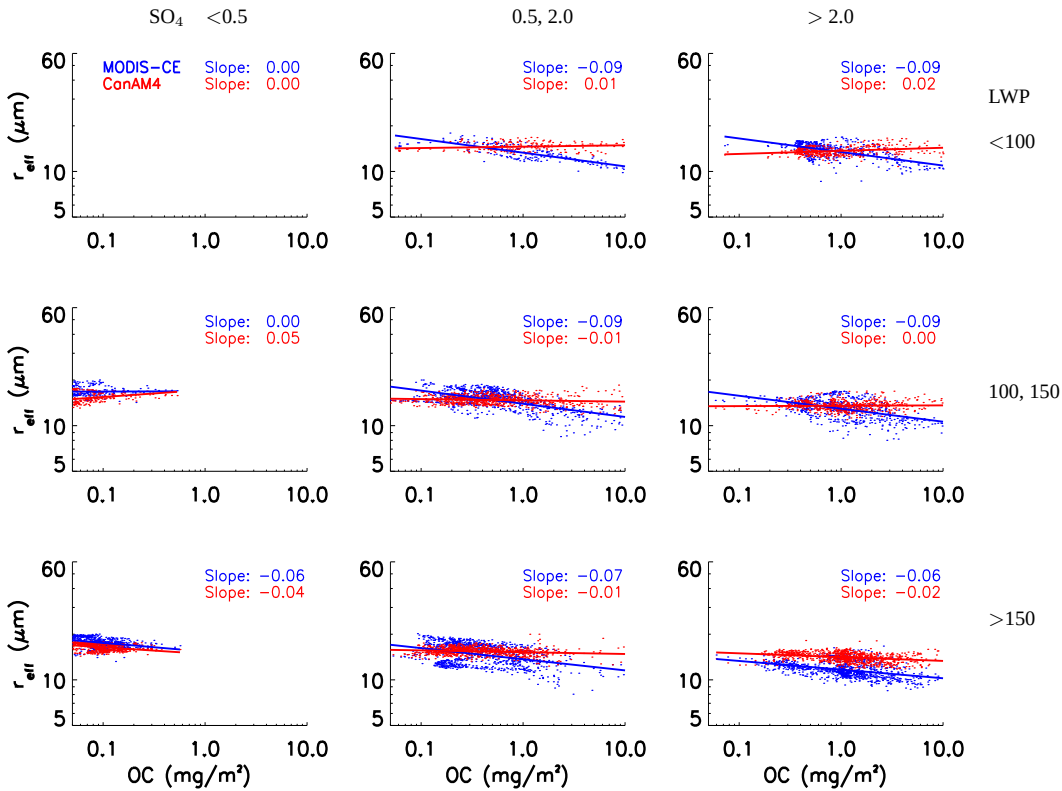

Fig. 5. Low (surface to 700 hPa) cloud effective radius (in μm) from MODIS-CE (in blue) and CanAM4 simulation (in red) versus hydrophylic organic carbon (OC) in JJA. The data were stratified for 3 categories of liquid water path (LWP, in g/m^2), and 3 categories of sulphate (SO_4, in mg/m^2). The slope from linear regression are also marked in the plots.

ACPD
10, 13945–13968, 2010

Constraints on first indirect effect of aerosols

X. Ma et al.

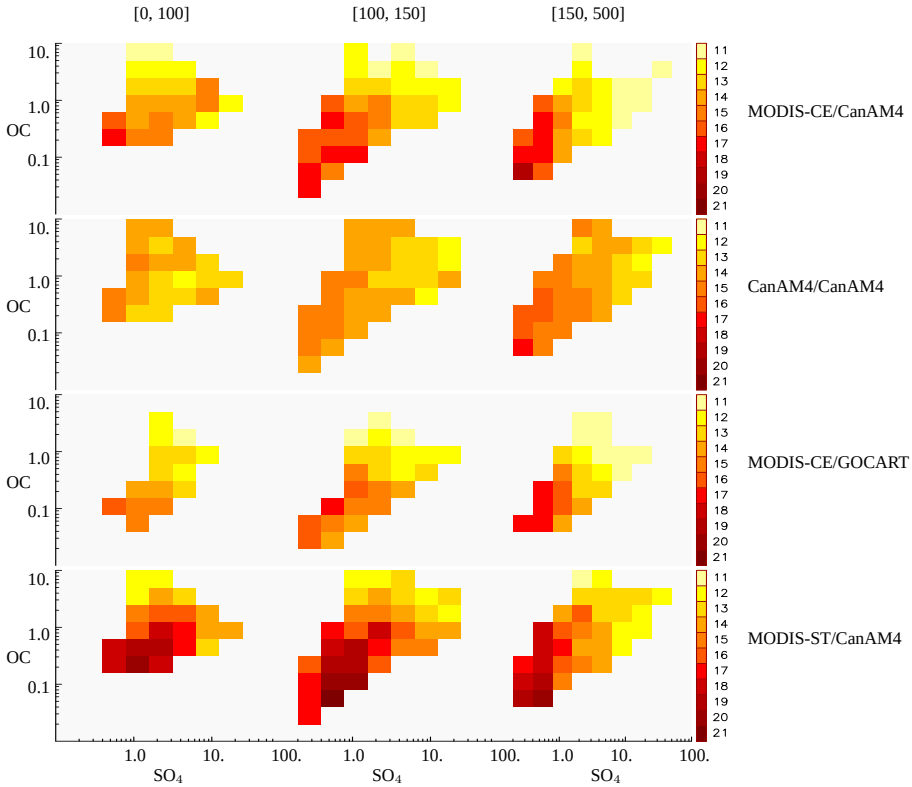

Fig. 6. Cloud effective radius (in µm) as a function of sulphate and organic carbon concentrations (units: mg/m^2). Results for effective radius from MODIS-CE (top panel), CanAM4 (second panel) using aerosol concentrations from CanAM4. Results for effective radius from MODIS-CE and simulated aerosol concentrations from GOCART, and the results for effective radius from MODIS-ST and simulated aerosol concentrations from CanAM4 are shown in the third and bottom panel, respectively. The data were stratified by using cloud liquid water path from CanAM4 simulations (columns, units: g/m^2).

ACPD
10, 13945–13968, 2010

Constraints on first indirect effect of aerosols

X. Ma et al.

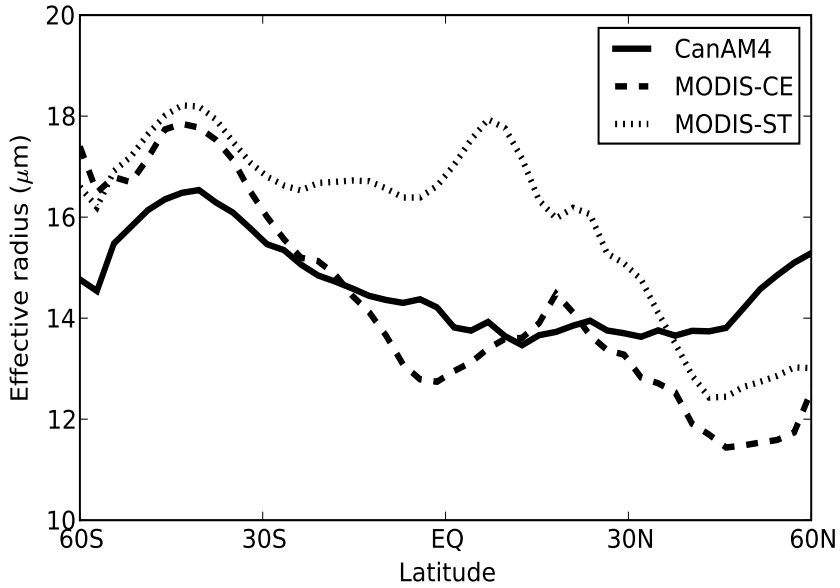

Fig. 7. Zonal mean cloud top effective radius in JJA from the CCCma CanAM4, MODIS-CE and MODIS-ST.

ACPD
10, 13945–13968, 2010

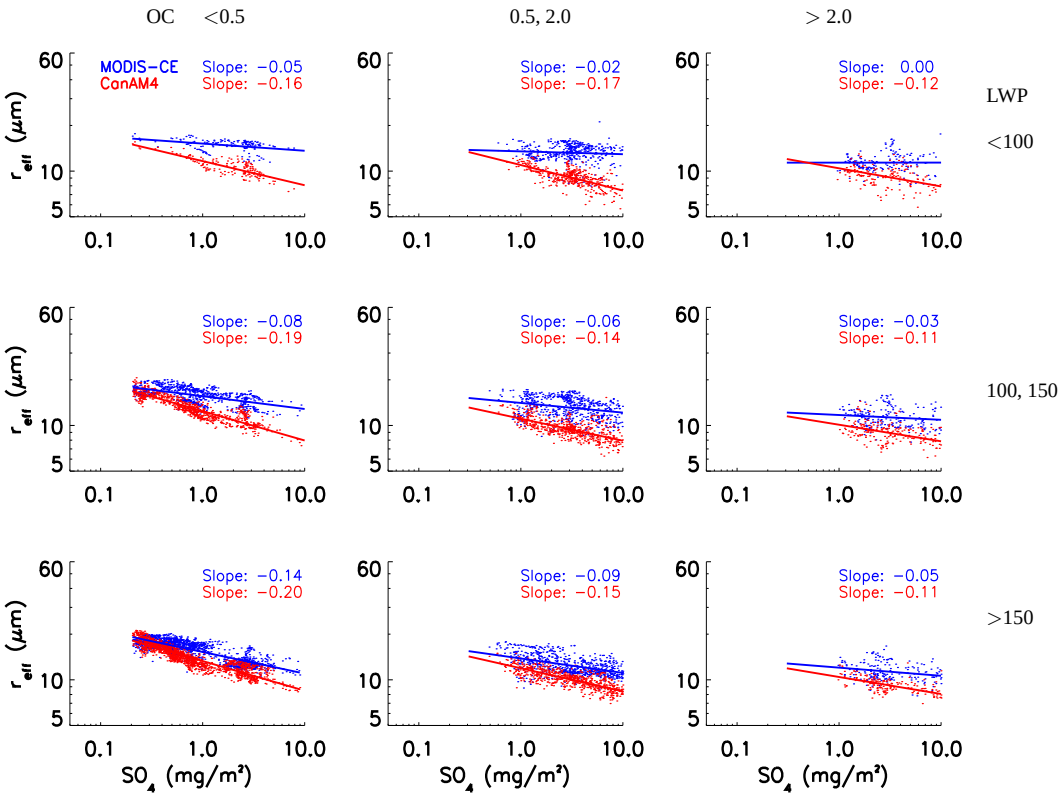

Fig. 8. Same as Fig. 4, but the simulation uses Menon's parameterization for CDNC.

ACPD
10, 13945–13968, 2010

Constraints on first indirect effect of aerosols

X. Ma et al.

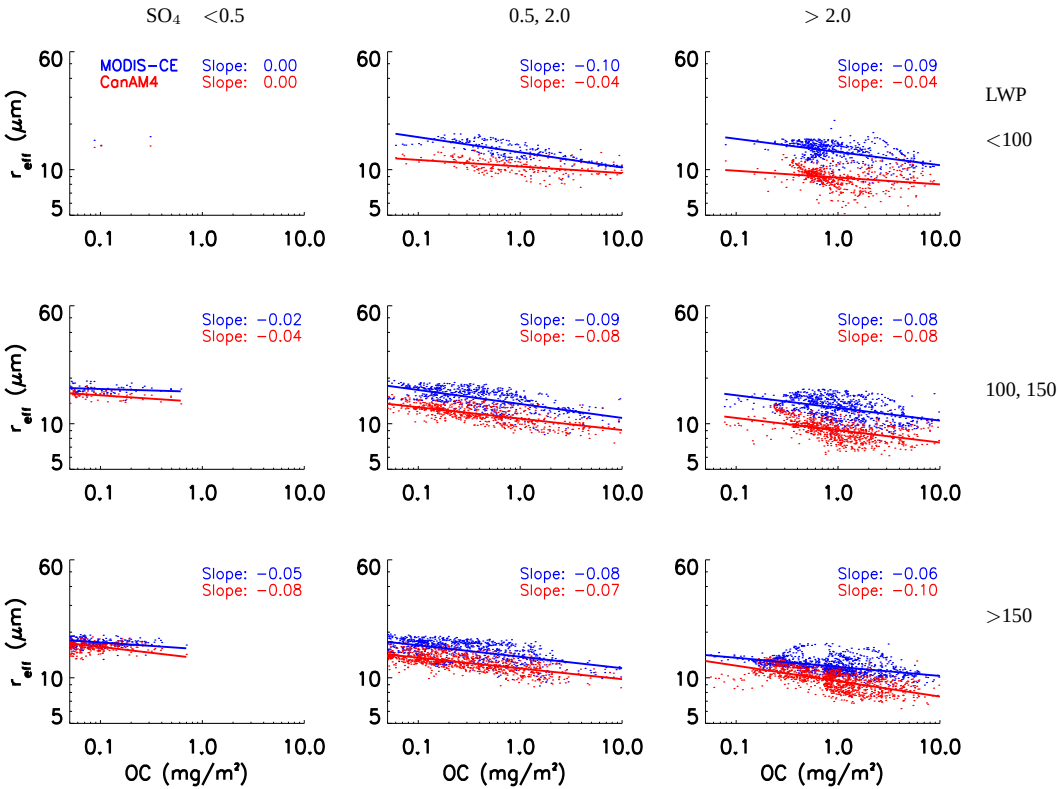

Fig. 9. Same as Fig. 5, but the simulation uses Menon's parameterization for CDNC.

ACPD
10, 13945–13968, 2010

Constraints on first indirect effect of aerosols

X. Ma et al.